Carpathian Journal of Earth and Environmental Sciences, August 2020, Vol. 15, No. 2, p. 347 – 358; Doi:10.26471/cjees/2020/015/135

NEW OCCURRENCES OF SULFATE MINERALS IN JIUL DE VEST UPPER BASIN, SOUTH CARPATHIANS, ROMANIA

Robert SZABO[1], Gheorghe C. POPESCU[1], Delia – Georgeta DUMITRAŞ[2], & Eduard GHINESCU[2]

[1]*Department of Mineralogy, Faculty of Geology and Geophisics, University of Bucharest, 1, Nicolae Bălcescu Blvd., Bucharest, robert21szabo@gmail.com, gheorghec.popescu@yahoo.com*

[2]*Geological Institute of Romania, 1, Caransebeş street, sector 1, Bucharest, d_deliaro@yahoo.com, ghinescu.edi@gmail.com*

Abstract: The study area is located in the western part of the Southern Carpathians, Romania. From a stratigraphical, morphological and geological point of view, it pertains to the Petroşani Basin, which is almost entirely crossed by Jiul de Vest River. Several occurrences of sulfates were identified in the upper basin of the river. The samples were collected from two perimeters, namely „Scocul Jiului" (P1) and „Tusu brook" (P2), located on the right tributary of the Jiu River. The sulfates discovered are water-bearing, pertaining to halotrichite - pickeringite isomorphic series, halotrichite and pickeringite being the main minerals observed, along with alunogen and gypsum. The sulfate minerals accompany pyrite micro-veins crossing metamorphic rocks (gneisses). The minerals were investigated using X-ray powder diffraction (XRD), infrared absorption spectrometry, micro-Raman spectrometry, scanning electron microscopy (SEM), combined with energy dispersion spectroscopy (SEM–EDS) and optical study. The chemical and textural complexity suggests the existence of minerals in the halotrichite - pickeringite isomorphic series, mixed in different proportions; alunogen and gypsum provided Raman and infrared spectra very close to those of synthetic samples in literature.

Keywords: sulfates, Jiul de Vest, halotrichite, pickeringite, isomorphic series, alunogen, gypsum, XRD, micro-Raman, infrared spectra.

1. LOCATION AND GEOLOGICAL SETTINGS

Jiul de Vest River crosses almost entirely the Petroşani Basin, located in Hunedoara County, Romania.

The researched area extends parallel to the flow direction of the river, from its springs to the point where it captures the waters of the Braia Brook, in Lupeni city (Fig. 1).

The basin is limited to the north by the southern part of Retezat Mountains and to the south by the northern branch of Vâlcan Mountains, both of them located in the west side of the South Carpathians.

The geology of the Jiul de Vest upper basin is built by formations belonging to the Danubian and Getic domains.

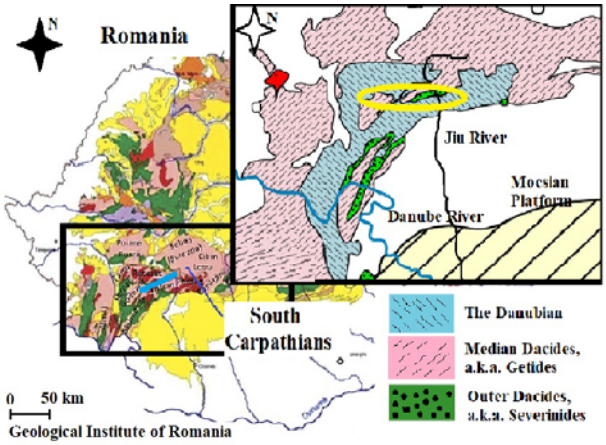

Figure 1. The studied area (highlighted with blue line and the yellow circle), South Carpathians, and the main geological structures (redrawn after the Geological Map of Romania and Balintoni et al., 2014)

In the study area, the formations belonging to the Getic domain appear as small blocks originating from the Getic realm, which was fragmented after the collision with the Danubian block (Popescu, 1981). The crystalline schists of the Lainici – Păiuş, Drăgşan and Sebeş - Lotru series, respectively, are part of the studied perimeter. Some formations belonging to the Severin domain also occurs, but no relations between these formations and the studied minerals were found in our research.

The studied area was divided in two perimeters namely P1, located in the region known as Scocul Jiului de Vest and P2, which corresponds to the left bank of Tusu Brook, the right tributary of Jiul de Vest River with confluence near the Lupeni city border. The geology of both perimeters is shown in the simplified maps presented in Figure 2, and 3, respectively, redrawn from Berza et al., (1984, 1986). The minerals identified in the Fe-rich alteration zones from P1 are gypsum, pickeringite, halotrichite, alunogen, pyrite, iron oxides and iron sesquioxides. In the P2 perimeter, the association of minerals comprises: gypsum, pickeringite, halotrichite, alunogen, pyrite and dolomite. See figure 2 and 3 marked with yellow stars.

The earliest formations that form the P1 fundament are assigned to the upper Precambrian and are represented by minor intrusions of granitoids belonging to the Prealpine unit of Retezat-Parâng, along with the Drăgşan Series (terrain) characterized by a Precambrian metamorphism (~ 800 Ma according to Balintoni et al., 2014).

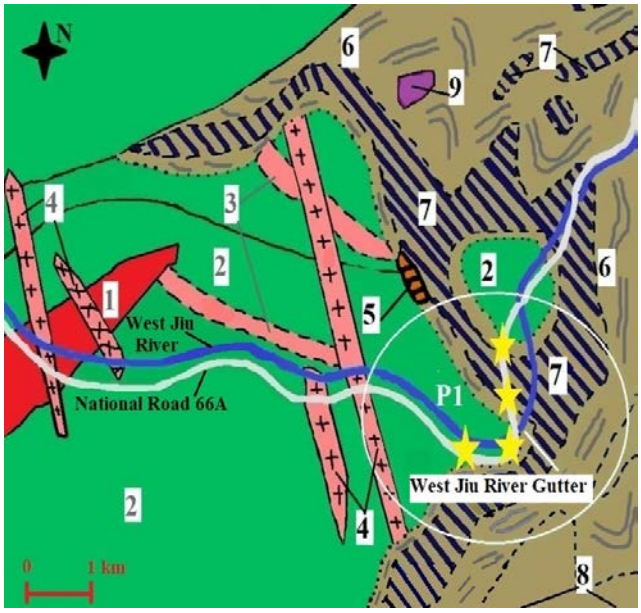

Figure 2 – Geological map of P1, Scocul Jiului de Vest (compiled after Berza et al., 1984): 1- Minor intrusions of granitoids, Upper Precambrian; 2 - amphibolites and amphibole-bearing gneisses +/-almandine, Upper Precambrian; 3 - gneisses with micas and plagioclase, Upper Precambrian; 4 - porphyry microgranites, lower Paleozoic; 5 - Valea Boului meta-arkoses with hematite concentrations, Lower Carboniferous; 6 - black sericite associated with graphite phyllites of Valea de Peşti, Lower Carboniferous; 7 - limestone and dolomite, Lower Carboniferous; 8 - metasiltites, metapsammites of Gârbovu, Lower Carboniferous; 9 - serpentinized or calcified peridotite, Neocomian - Tithonic.

In P1 there are isolated outcrops of serpentinized or talcized peridotites belonging to the Severin Domain (the Severinides), assigned to the Tithonic – Neocomian age (Berza et al., 1984).

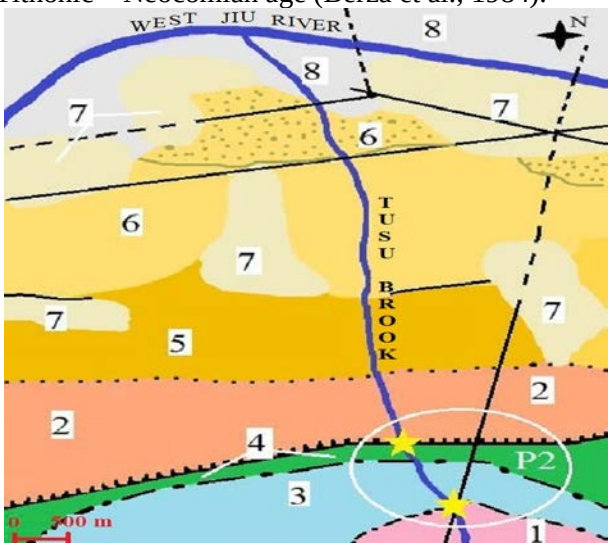

Figure 3. – Sketch of the geological map of P2, Tusu River Valley (compiled after Berza et al., 1986): 1 - biotitic gneisses, upper Precambrian; 2 - micaceous gneisses with plagioclase, amphibolites and serpentinites of Sebeş-Lotru series, Upper Precambrian; 3- conglomerates, sandstones, black clays +/- chloritoid, Schela formation, Lower Jurassic; 4 - bioclastic, micritic, pelitic, recrystallized limestones of Lupeni, Late Jurassic-Lower Cretaceous; 5 - red rocks, sandstones and conglomerates (the red Rupelian horizon); 6 - sandstones, micro-conglomerates, conglomerates and clays with intercalations of sandstones, shale and coal (the Chattian productive horizon); 7- sands and gravels (Pleistocene); 8 - alluvial meadows (Holocene).

P2 comprises sequences of micaceous gneisses with plagioclase, amphibolites and serpentinites, representing the undifferentiated Sebeş-Lotru series, amphibolites and amphibole gneisses known as the Straja formation and amphibolites belonging to the Drăgşani series. All these formation are of Precambrian age (e.g., Balintoni et al., 2014).

The Mesozoic is represented by conglomerates, sandstones, clays +/-anthracite +/-chloritoid assigned to the Schela formation (Popescu and Constantinescu, 1982), characterized by a

dynamic alpine anchimetamorphism; the bioclastic, micritic, pelitic, crystalline limestone, known as the Lupeni limestones, are assigned to the boundary between upper Jurassic and lower Cretaceous.

The youngest formations are attributed to the Rupelian, Chattian and Quaternary ages of the Petroşani Basin. The Rupelian is represented by red rocks, sandstone and conglomerates, forming the red horizon specific to the Petroşani basin. The Chattian is made up of two productive horizons consisting of clays with intercalations of sandstones, shales and coal deposits, and the gray horizon formed by sandstone, micro-conglomerates and conglomerates. The quaternary is represented by the fluvial deposits of upper and lower terraces and alluvial meadows (Berza et al., 1986).

Previous studies have been undertaken by authors regarding the study of the sulfate group minerals and the process of identification. The previous researches are based on X-Ray powder diffraction, Raman spectrometry, Scanning Electron Microscopy with Energy Dispersive Spectroscopy (SEM - EDS). These type of analytical methods were used in our paper to in order to identify and separate the sulfates.

Researches on alunogen were made by Fang & Robinson (1976), Košek et al., (2018); halotrichite was studied along time by Brant & Foster (1959), Cody & Brigss (1973), Lovas (1986), Frost et al., (2005), Ballirano (2006), Locke et al., (2007), Palmer et al., (2011); Gypsum by Hass & Sutherland (1956), Dumitraș (2009); Pickeringite by Quartieri et al., (2000), Palmer & Frost (2006). Of course, there are many other papers done by different researchers on the globe. The ones mentioned before are considered important by the authors because they present data obtained by various analytical methods, especially diffraction, infrared and micro-Raman.

The main goal of our paper is to separate the minerals discovered on the northern flank of Vâlcan Mountains. For example, pickeringite forms a solid solution with halotrichite, these two minerals being intimately linked and the mechanical separation is very difficult sometimes impossible. The other two minerals discovered are easier to identify.

Characteristic to our research is that these sulfate minerals were not found on waste dumps, or in open pits, neither in caves. The minerals found by us are the result of supergene alteration, formed through oxidation of common sulfides especially pyrite micro-veins exposed to precipitation.

In the study area, this is the only situation known, where these minerals occur naturally in an open environment.

2. ANALYTICAL METHODS

The samples took off were investigated using a combination of methods including X-ray powder diffraction (XRD), infrared absorption and micro-Raman spectrometry, scanning electron microscopy combined with energy dispersion spectroscopy (SEM–EDS) and optical study.

The X-ray powder-diffraction (XRD) analysis was performed on a Bruker D8 Advance automated diffractometer equipped with a vertical goniometer, configuration θ - 2θ, with Cu radiation and Ni filter. The operating voltage was 40 kV and the beam current was 40 mA. Diffraction patterns were recorded from 5 to 90° 2θ, with a step scan of 0.02° 2θ, at 1 s per step. The receiving slit was 0.6 mm, in a slit system of 1-0.1-1. The counting time was 4 s per step, for a step size of 0.01° 2θ, and data were collected from 4 to 90° 2 θ. The unit-cell parameters were calculated by the least-squares refinement of the XRD data, using the computer program of Appleman & Evans (1973).

The infrared absorption spectrum was recorded with a Bruker Tensor 27 spectrometer, using a standard pressed-disk technique, after embedding approximately 0,148 mg of mechanically grounded sample in approximately 0,0024 mg of dry KBr and compacting under the equivalent of 9 tons of pressure. The micro-Raman analysis was made with the help of a Renishaw In Via Raman apparatus, equipped with two lasers with wavelengths of 532 nm and 785 nm, with a maximum power of 50 mW and a CCD detector. The analyzes were performed with the Renishaw inVia micro Raman spectrometer, with the following general characteristics: 532 nm wavelength laser with a 1800/nm holographic gauge at a 10% capacity and an exposure time of 3 – 5 s, acquisition time of 20 – 30 s, using a Leica microscope with 50X lens, attached to the spectroscope. For the current study the following parameters were used in the analysis: the laser was set to 542 nm edge with power 5%, grating: 1800 l/mm (VIS), objective from 5X magnification to 50X magnification, scan type used were both continuous and static scan, focus mode was regular, and the spectral range 100.83 to 4002.28 (centre - 1111) Raman shift / cm^{-1}, exposure time from 10 seconds to 15 and even 20 on different probes. No degradation was observed due to the stability of the minerals.

The scanning electron microscopy combined with energy dispersion spectroscopy (SEM–EDS) was performed with a Hitachi TM 3030 Plus Tabletop SEM equipped with a Bruker Quantax X Flash® 6/10 detector.

The samples taken from nature were analysed with the binocular lens, were cleaned and separated, after were grinded mechanically and turned into pressed powder pellets accordingly. Some of the grains were saved and reduced to a smaller size to study their preliminary chemistry with the help of the SEM-EDS apparatus.

X-ray powder diffraction analyses were done at the same time and on the same pellets along with Infrared analyses (FT-IR). The last type of analysis done was the micro -Raman.

The optical study was done using both a Leitz Wetzlar microscope and an Optika B-Pol microscope. The images of thin sections were captured using a PANPHOT Leitz Wetzlar microscope equipped with a Nikon Eclipse E-400 40W photo camera.

3. MINERAL DATA

The main sulfates identified in the area are part of the hydrous sulfate category, most of them being terms of the halotrichite - pickeringite solid solution series. Gypsum and alunogen were also found. Around 20 samples were taken off from the field in the two perimeters. Samples were identified, for example, as VJV01 where VJV means „Valea Jiului de Vest" (the West Jiu Valley), and „01" is the number of the sample.

3.1. Pickeringite

Pickeringite, with ideal formula $MgAl_2(SO_4)_4 \cdot 22H_2O$ (Figs. 4 – A, B) is the magnesian end-member of the halotrichite - pickeringite solid solution series. It was identified in both investigated perimeters, in association with halotrichite terms.

Both on-field and microscopic observations show that the mineral occurs as fibrous aggregates up to 2 mm in length. The color ranges from yellowish-white in P1 to yellow in P2. A silky luster was observed. It is fractured in an uneven pattern; the flat surfaces present no cleavage. The crystals observed in the two perimeters are biaxial negative, being elongated after the c* axis.

X-ray powder diffraction analyses allow the identification of pickeringite in 4 samples (VJV01, VJV02, VJV06 and VJV07). In each of the 4 samples, the pickeringite appears intimately associated with halotrichite terms.

The average unit-cell parameters, taken as mean of the values obtained by least-squares refinements from 4 sets of X-ray powder data including reflections unequivocally attributable to pickeringite, using the computer program of Appleman and Evans (1973) modified by Benoit (1987) are: a = 6.182(4) Å, b = 24.274(5) Å, c = 21.226(4) Å, β = 100.25(3)º and V = 3134.33(5) Å^3. The obtained values are very close to those in literature (Table 1).

The indexing of the four diffraction patterns of the samples containing pickeringite was done taking into account the monoclinic symmetry of the mineral, space group P21/b.

Table 1 – Comparison between the average cell parameters of the pickeringite

Authors	a (Å)	b (Å)	c (Å)	β(o)
Present study	6.182 (4)	24.274 (5)	21.226 (4)	100.25 (3)
Quartieri et al., (2000)	6.1844(2)	24.2715 (9)	21.2265 (7)	100.32 6(4)
Anthony et al., (1990)	6.184 (2)	24.2715 (9)	21.2265 (7)	100.32 6(4)
Ballirano (2006)	6.187 (1)	24.2549 (6)	21.2297 (5)	100.32 2(1)
Lafuente et al., (2015) RRUFFID R060108.2	6.18 (1)	24.268 (4)	21.217 (4)	100.31 (1)

Pickeringite and halotrichite terms of the pickeringite – halotrichite solid solution series occur in intimate mixtures; this led to the impossibility of separating them at the binocular microscope. Splitting of the main reflections occurs in most of the XRD patterns recorded for pickeringite – halotrichite terms, being indicative for the presence of both pickeringite and halotrichite.

For pickeringite, the most important three reflections occur at 4.82 Å (I = 100), 3.51 Å (I = 90), and 4.32 Å (I = 35).

The Fourier-transform infrared absorption spectrometry analyzes (FT-IR) revealed bands specific to S-O and O-H-O bonds in the pickeringite structure.

The study of the infrared absorption spectra of pickeringite samples shows that in the region of the fundamental stretching of water (3000 to 4000 cm^{-1}), shows two resolute absorption bands at about 3422 cm^{-1} and 3382 cm^{-1}, characteristic for the ν_3 and ν_3' antisymmetric stretchings of water, as well as a third band, at about 3040 cm^{-1}, pertaining to the ν_1 symmetric stretching of H-O-H groups. These bands can be correlated with the hydrogen bridges established between the water molecules in the

structure. If we take into account the O-H-O distances in the structure (Palmer et al., 2011) and apply the equation of Libowitzky (1999) correlating the frequency of bands with the O-H-O interatomic distance, the water bands of the pickeringite structure should occur between 3500 cm^{-1} and 3000 cm^{-1} (Frost et al., 2005). As can be seen, the values obtained are perfectly consistent with the position of the water stretching bands in our spectra. The in-plane bending band characterizing the water molecule was identified at approximately 1640 cm^{-1}.

In the spectral range between 1500 cm^{-1} and 600 cm^{-1} the bands identified are characteristic for the vibrations of the sulfate groups in the structure. The bands identified are those at 1098 cm^{-1} and 1080 cm^{-1} (ν_3 and ν_3' antisymmetric stretchings O-S-O, respectively), 980 cm^{-1} (ν_1 symmetric stretching), and 609 cm^{-1} (ν_4' in-plane bending), respectively. Two of the absorption bands which occur at values less than 600 cm^{-1} (at about 470 cm^{-1} and 440 cm^{-1}) could represent the ν_2 and ν_2' out-of-plane bending modes of the sulfate groups (Nakamoto, 2006).

Micro-Raman spectrometric analyzes performed on pickeringite samples revealed the presence of two high intensity bands: one around 980 cm^{-1}, assigned to the ν_1 symmetric stretching mode of sulfate groups, and one around 970 cm^{-1} which represents a water vibrational mode (Palmer & Frost, 2006).

At values less than 650 cm^{-1}, the spectra show bands characteristic of Mg-O vibrations, assumable to ionic bonds.

The main such bands were observed at 611 cm^{-1}, 463 cm^{-1}, 423 cm^{-1} and are similar to those reported by Frost et al., (2005), (Table 2).

Table 2. Comparative values of Raman bands for pickeringite (cm^{-1})

Pickeringite, Jiul de Vest Basin	halotrichite-pickeringite Frost et al., (2005)	Synthetic pickeringite Palmer and Frost, (2006)
611	624, 605	611
463	466	459
423	422	445, 366

In addition to the methods described above, SEM-EDS analyses were performed. SEM images show the presence of pickeringite crystals elongated along the c* axis (Fig. 8, A, B). EDS analyses revealed the presence of magnesium, aluminum, sulfur and oxygen.

The result of a representative analysis is given in Table 3, whereas the elemental composition is depicted in Figure 4.

Table 3. Representative chemical composition of pickeringite (sample VJ06.1)

Element VJ06.1	norm. C [wt.%]	Atom. C [at.%]	Error [%]
Oxygen	77.17	86.08	10.3
Sulfur	13.52	7.53	0.6
Aluminum	6.09	4.03	0.3
Magnesium	3.22	2.36	0.2
Total	100.00	100.00	

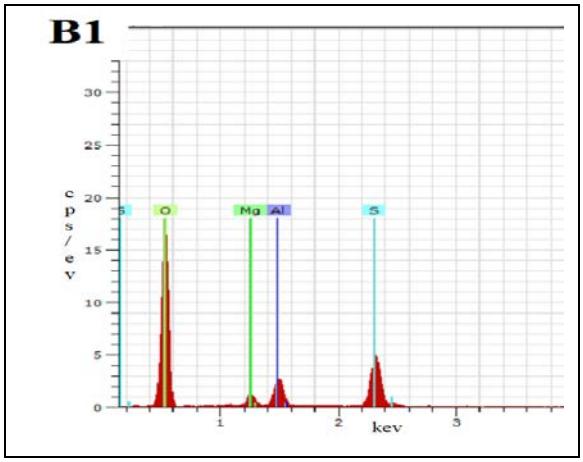

Figure 4. SEM-EDS chemical analysis, on a representative sample of pickeringite (VJV06.1 in P1)

3.2. Halotrichite

Halotrichite, ideally $FeAl_2(SO_4)_4 \cdot 22H_2O$, is the iron end-member of the halotrichite - pickeringite solid solution (isomorphic) series. It was identified in the both investigated perimeters, in different percentages, being always associated with pickeringite.

The mineral occurs in fibrous masses, having a green to pale green color. The luster is silky. Individual crystals are needle-like, with developments of up to 1 mm in length.

X-ray powder diffraction analyzes made possible to identify halotrichite terms in 2 samples (VJV03 and VJV04). In both of the samples the mineral appears intimately associated with pickeringite.

The indexing of the diffraction patterns was done taking into account the monoclinic symmetry of the mineral, in the same space group as for pickeringite ($P2_1/c$).

Theaverage unit-cell parameters, taken as mean of the values obtained by least-squares refinements from the 2 sets of X-ray powder data including reflections unequivocally attributable to halotrichite, are: a = 6.182(7) Å, b = 24.225(8) Å, c = 21.056(6) Å, β = 100.62(3)º and V = 3102.2(3) Å^3. These values are quite close to those in literature (Table 4).

Table 4 – Comparison between the average cell parameters of halotrichite

Authors	*a* (Å)	*b* (Å)	*c* (Å)	*β* (o)
Present study	6. 182(7)	24. 225(8)	21. 056(6)	100. 62(3)
Lovas G.A., (1986)	6.1954 (7)	24.262 (3)	21.262 (2)	100.3 (1)
Ballirano (2006)	6.1909 (3)	24.264 (11)	21.2595 (11)	100.274 (3)
Lafuente et al., (2015) RRUFF- ID R0601 18.1	6.184 (1)	24.257 (3)	21.230 (2)	100.333 (8)

For halotrichite, the principal three reflections occur at 4.78 Å (I = 100), 3.484 Å (I = 75), and 6.02 Å (I = 35).

As well as for pickeringite, the FT-IR spectra clearly show absorption bands due to molecular water, namely the broad OH-stretching having distinctive bands at 3449 cm^{-1} and 3364 cm^{-1}, and the broad absorption maximum at 1645 cm^{-1}, assigned to the H-O-H "scissors" bending vibration. Water librations are materialized by bands recorded at ~1401 cm^{-1} and 921 cm^{-1} also reported by Ross (1974).

In the spectral range between 1500 cm^{-1} and 600 cm^{-1}, the main bands are characteristic for the vibrations of the sulfate groups in the structure.

The bands identified are those at 1099 cm^{-1} (ν_3 antisymmetric stretching O-S-O), 975 and 920 cm^{-1} (ν_1 and ν_1' symmetric stretchings), and 693 and 611 cm^{-1} (ν_4 and ν_4' in-plane bending), respectively. Apparently, in halotrichite, both the symmetric stretching and in-plane bending are double degenerate.

Two of the absorption bands which occur at values less than 600 cm^{-1} (at about 470 cm^{-1} and 440 cm^{-1}) could represent the ν_2 and ν_2' out-of-plane bending modes of the sulfate groups. Both FT-IR and micro-Raman analyzes showed the presence of a strong symetric stretching band characteristic to sulfate groups at 975 cm^{-1} (Raman and IR active) and at 995 cm^{-1} respectively (Raman active).

Note, however, that pickeringite and halotrichite terms are notoriously difficult to separate. The continuous substitution between Fe^{2+} and Mg^{2+} atoms prevents the record of Raman and FT-IR spectra corresponding to the end-members of the pickeringite – halotrichite series, compositions corresponding to the two minerals being found together in all the analyzed samples.

Note, however, that in our separates, pickeringite crystals have glued fine needles of halotrichite. The values obtained from analyzes carried out on samples from the Jiu Valley show the presence of halotrichite in most of these (Table 5).

Table 5. Raman bands recorded for halotrichite (cm^1)

Halotrichite samples from Jiul de Vest basin	Natural halotrichite (Palmer and Frost, 2006)
3271	3255
1142	1148
1079	1070
995	995
975	975
614	622
528	529
463	468
422	424
308	314

3.3 Alunogen

Alunogen, ideally $Al_2(SO_4)_2 \cdot 17H_2O$, was found in both P1 and P2 areas and occurs as small tabular crystals forming fibrous masses or crusts. Small, semi-transparent, isolated crystals and massive aggregates were also observed.

The mineral has white to yellowish - yellow colors in P2 while in P1 the color is yellow and sometimes appears with pronounced orange tints. The mineral is optically positive.

X-ray powder diffraction analyzes made possible to identify alunogen in one sample (VJV03.1), in which the mineral appears intimately associated with pickeringite.

After indexing the resulting diffraction patterns in the hypothesis of the triclinic symmetry, space group *P*-1 of the mineral, the cell parameters obtained by least squares refinement, using the computer programs stated before, are: a = 7.421(9) Å, b = 26.917(7) Å, c = 6.053(8) Å, α = 89.95(3)º, β = 97.04(6)º, and γ = 91.21(4)º.

These values, obtained for the alunogen identified in the Western Jiu Valley formations, are very close to the data in literature (Table 6).

For alunogen, the principal three reflections occur at 4.48 Å (I = 100), 4.39 Å (I = 81), and 4.32 Å (I = 81).

Both on FT-IR and micro-Raman analyses revealed as main bands those characteristic for vibrational modes of sulfate groups and molecular water. The bands attributable to the stretching vibrations of water occur between 3600 cm^{-1} and 2300 cm^{-1} (Košek et al., 2018). These bands are also Raman-active; in the Raman spectrum these bands occur at 3406 and 3267 cm^{-1}, respectively (Table 7). The corresponding bending vibration of water is IR-active and occur in our spectrum (not given, but available by request from the first author) at about 1600 cm^{-1}. A libration of water, materialized by a

weak-intensity band recorded at about 1400 cm^{-1}, can be attributed to additional water molecules in impurities, e.g., admixed pickeringite.

Table 6. Average cell parameters for alunogen

Authors	***a* (Å)**	***b* (Å)**	***c* (Å)**	***α*°**	***γ*°**
Present study	7.421 (9)	26.917 (7)	6.053 (8)	89.95 (3)	91.21 (4)
Fang & Robinson (1976)	7.420 (6)	26.97 (2)	6.062 (5)	89.57 (5)	91.53 (5)
Žáček (1988)	7.423 (3)	26.96 (1)	6.049 (4)	89.97 (4)	91.79 (1)
Košek et al., (2018)	7.425 (1)	26.936 (2)	6.057 (1)	89.90(2) 89.99(2)	91.95(1) 91.87(1)
Lafuente et al., (2015) RRUFF-ID R060015.1	7.413 (3)	26.722 (8)	6.021 (7)	88.728 (3)	91.802 (5)

Table 7. Raman bands recorded for alunogen (cm^{-1})

Alunogen from the Jiul de Vest, Basin VJV03.1	Alunogen (Košek et al., 2018)	
	Synthetic alunogen	Natural alunogen
3406	3440	3351
3267	3240	3260
1144	1126	1127
1083	1083	1089
992	992	992
612	612	612
463	469	470
305	308	310
219	278	180
132	136	138

Two other prominent bands occur, on the infrared spectra, at 974 cm^{-1} (O-S-O stretching or O-H libration) and at 920 cm^{-1} (O-H libration), respectively (probably due to an impurity). Košek et al., (2018) observed similar values in an alunogen sample originating from the Czech Republic.

Vibration modes of sulfate groups in the structure are better presented by the Raman spectrum, which shows the presence of a strong vibration band at 992 cm^{-1}, v_1 the O-S-O stretching. This vibration is Raman active and triply degenerate to this vibration being recorded at 1083 cm^{-1} which represents the v_3 and the 1144 cm^{-1} which is the doublet in this case.

At low frequencies, the v_4 in-plane bending of sulfate groups is materialized by a band recorded at 463 cm^{-1}, whereas a band recorded at 305 cm^{-1} can represent a bending mode of water.

The XRD analyzes carried out on samples taken off from Jiul de Vest River, from both P1 and P2 study areas show that alunogen is admixed with a halotrichite – pickeringite term. Some of the Raman-active vibration modes could consequently result in composed bands pertaining to two mineral species.

In addition to the methods described above SEM-EDS analyses were performed (Table 8). SEM images show the presence of alunogen crystals elongated along the [001] axis (Fig. 5, E). EDS analyses revealed the presence of aluminum, sulfur and oxygen in alunogen along with some traces of magnesium, which probably originate in the admixed pickeringite.

Table 8. Representative chemical composition of alunogene (sample VJV04.1)

Element	norm. C	Atom. C	Error
	[wt.%]	[at.%]	[%]
Oxygen	42.87	61.95	5.0
Sulfur	29.39	21.13	0.8
Aluminum	16.40	6,80	0.4
Magnesium	3.79	3.60	0.2
Total	100.00	100.00	

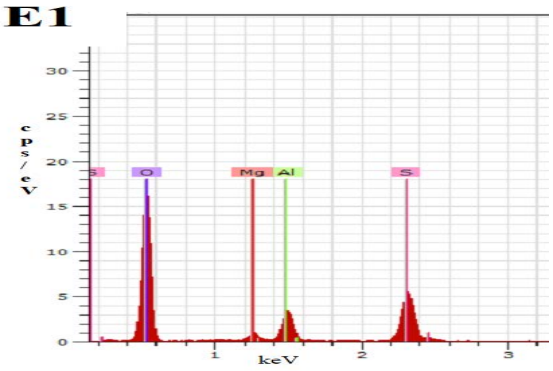

Figure 5. SEM-EDS chemical analysis of one sample of alunogen found in P2 (VJV03.1 (E1)

3.4. Gypsum

Gypsum (ideally $CaSO_4 \cdot 2H_2O$) was found in both P1 and P2 study areas. The mineral occurs as small, generally translucent crystals, between 0.01 mm and 2 mm in length. Individual crystals are flattened on {010} and elongated toward [001]. Stacking aggregates of crystals grown subparallel or parallel to (010) are common.

X-ray powder diffraction analyzes revealed the purity of two samples from P2 (VJV05.1 and VJV05.2). The average values of the unit cell

parameters calculated for these representative samples are presented in table 9, together with similar values reported in the literature.

Table 9. Unit-cell parameters of selected samples of gypsum

Authors	*a* (Å)	*b* (Å)	*c* (Å)	β (o)
This study	5.691 (1)	15.159 (1)	6.519 (2)	118.34 (7)
Atoji & Rundle (1958)	5.680 (8)	15.180 (9)	6.520 (8)	118.38 (33)
Cole & Lancucki (1973)	5.670 (2)	15.201 (2)	6.533 (2)	118.60 (7)
Pedersen & Semmingsen (1982)	5.679 (5)	15.202 (14)	6.522 (6)	118.43 (4)
Innorta et al., (1980)	5.677 (7)	15.187 (40)	6.527 (7)	118.39 (5)
Diaconu et al., (2008)	5.674 (2)	15.188 (5)	6.510 (3)	118.34 (2)
Dumitraș (2009)	5.680 (8)	15.194 (35)	6.514 (11)	118.33 (1)
Lafuente et al., (2015) RRUFF ID R060509	5.670 (5)	15.199 (1)	6.521 (6)	118.42 (1)

Table 10. Infrared absorbtion bands recorded for a gypsum sample from Jiul de Vest basin (cm^{-1})

Structural group	Vibrational mode	Sample VJV05.1	Intensity, character*
H_2O	H-O-H antisymmetric stretching (ν_3)	3550	m, b
H_2O	H-O-H antisymmetric stretching (ν_3')	3405	m, s
H_2O	H-O-H in-plane bending (ν_4)	1686	w, b
H_2O	H-O-H in-plane bending (ν_4')	1621	m, s
$(SO_4)^-$	O-S-O antisymmetric stretching (ν_3)	1144	s
$(SO_4)^-$	O-S-O in-plane bending (ν_4)	669	m, s
$(SO_4)^-$	O-S-O in-plane bending (ν_4')	603	m, b

* s = strong; m = medium; w = weak; vs = very strong; s = sharp; b = broad.

Table 10 shows the frequencies, character and intensity of the infrared-active absorption bands characteristic for the gypsum samples, together with an attempt to assign these bands to a specific vibration. The main IR-active vibrations depicted in the FT-IR spectra pertain, as expected, to molecular water and sulfate groups. As concerning the molecular water, this is hydrogen-bonded (*e.g.*, Pedersen & Semmingsen, 1982). Using the equation proposed by Libowitzky (1999), correlating the stretching frequencies to the interatomic distance O-H-O, the two water bands of the gypsum structure should occur between 3509 cm^{-1} and 3318 cm^{-1}, which is fully proved by our records (Table 11). The in-plane bending of molecular water is, on its turn, double degenerate, the two bands marking this vibration (ν_4 and ν_4' in Table 11) occurring at frequencies close to those detected by Seidl et al., (1969) for synthetic gypsum: 1686 cm^{-1} and 1621 cm^{-1}, respectively.

The antisymmetric stretching (ν_3) of sulfate groups is both infrared and Raman active, and is double degenerate. The corresponding bands occur at 1144 cm^{-1} and 1121 cm^{-1} in the infrared spectra (Table 11), the last one being perceived as shoulder of the broad complex of bands that materializes the sulfate antisymmetric stretching.

The in-plane bending of sulfate groups is also double degenerate and is materialized by the bands recorded at 669 and 603 cm^{-1} (e.g., Dumitraș, 2009).

The Raman spectrum (Table 11) is also dominated by the presence of sulfate bands, as follows:

Table 11. Raman bands recorded for gypsum (cm^{-1})

Gypsum from Jiul de Vest, P2	Gypsum (Buzgar et al., 2009)
1134, 1106	1143
1007	1010
669	674
620	622
491	495
412	416
	316
219	
179	

The water content of the gypsum raises some problems in the case of the minerals found in the West Jiu Valley. In the case of ν_3, the values are up-shifted following the decrease of the hydration degree, from anhydrite to bassanite and finally gypsum (Apopei et al., 2014).

The signal at 1106 peak also mentioned in Buzgar et al., 2009, can be attributed to bassanite or maybe anhydrite.

However, in our study, the infrared spectrum and the XRD analysis along with the SEM-EDS analysis have clearly shown the presence of gypsum. The signals for bassanite and anhydrite may be the result of the evolution in nature between these minerals, finally gypsum being the one that captured the water molecule.

Plate I

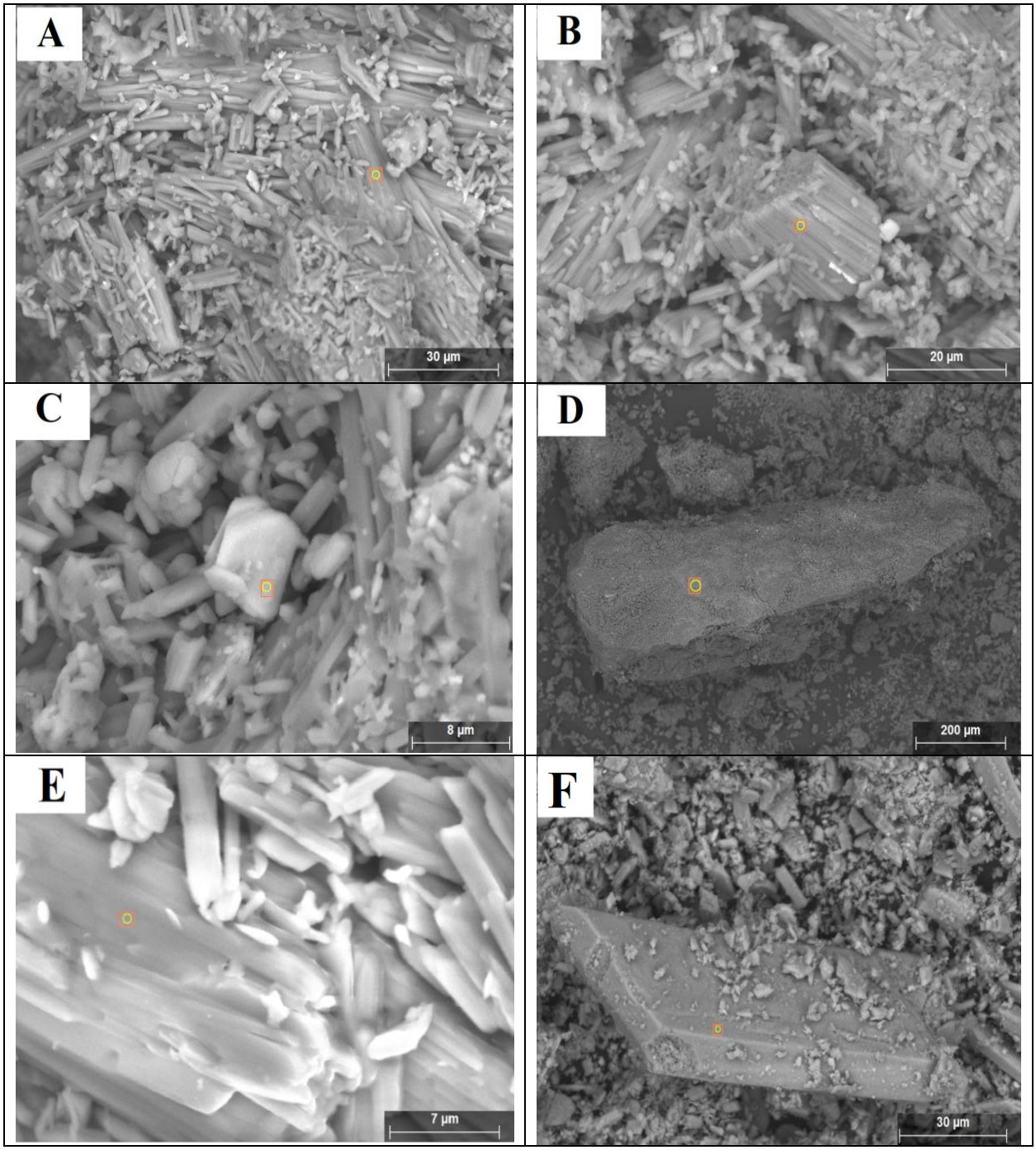

SEM photographs of representative sulfate samples: Back scattered electron (BSE) for two representative samples of pickeringite VJ02.8 (A) and VJ06.1 (B), in which clusters of crystals elongated after the c* axis can be observed; halotrichite VJV04.1 (C) and VJV04.2 (D) with singular monoclinic crystals elongate after the [001] axis; Back scattered electron (BSE) image of a sample of alunogen VJV03.1 (E), in which a large crystal can be observed. Along with small broken crystals of pickeringite, flattened gypsum crystals developed along the [010] axis and platy on (001) such as in sample VJV05.1 (F).

The ν_1 vibrations have the same trend. The general cause for the systematic shift of Raman peaks are the existing variations in the structure of covalent bonded ionic groups. The in-plane bending is, on its turn, double degenerated and materialized by a couple of bands located at 669 cm^{-1} (ν_4) and 620 cm^{-1} (ν_4'), respectively. The out-of-plane bending is also double degenerate and evidenced by two bands recorded at 491 cm^{-1} (ν_2) and 412 cm^{-1} (ν_2'), respectively. As well as the XRD analyses, the

multiplicity of bands obtained by the Raman spectra characterizes pure gypsum, close to stoichiometry.

This conclusion is also supported by the SEM-EDS analyzes, which revealed the presence of calcium, sulfur and oxygen as sole elements (Figs. 6 – F, G; Table 12). The elemental Kα lines are shown in Fig. 7.

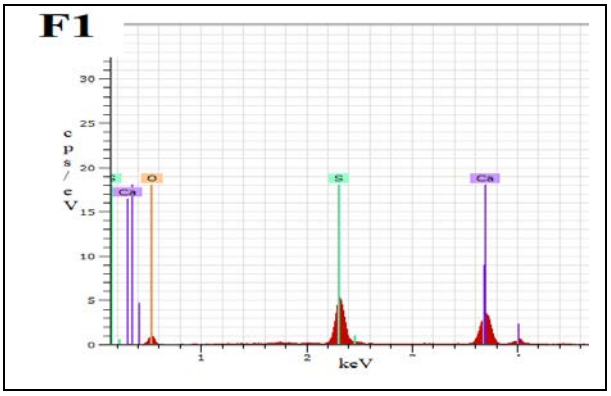

Figure 6. SEM-EDS analysis of gypsum (sample VJV05.1, F1)

Table 12. Chemical composition for gypsum (sample VJV05.1, F1)

Element	norm. C	Atom. C	Error
	[wt.%]	[at.%]	[%]
Oxygen	35.49	55.20	5.1
Sulfur	30.58	23.23	0.9
Calcium	33.93	21.07	0.8
Total	100.00	100.00	

4. CONCLUSIONS

Four minerals pertaining to sulfate class were identified during the field study occasioned by this work: halotrichite, pickeringite, alunogen and gypsum. These minerals are not cave minerals, as most of the sulfates described in Romania, nor were formed in former quarries or tailing dumps resulting from mining operations and affected by weathering. The formation of sulfates in the Jiul de Vest basin was due to the weathering of pyrite micro-veins, exposed to the action of meteoric water. The host rocks, also influenced by weathering, are metamorphic rocks, especially quartz-feldspar rocks, which were a potential source for Ca in the gypsum network and for Al and Fe in other sulfates.

As regards pickeringite terms, they are intimately associated with halotrichite ones, association that occurs in all of the studied perimeters. The two minerals form an isomorphic series, pickeringite terms occurring as a result of larger Mg availability in the system. Halotrichite is the product resulting from the action of aluminum-rich sulfate solutions that fixed iron ions originating from pyrite, catalyzed by a small amount of oxygen (Mastacan & Mastacan, 1976). Iron comes from pyrite, while the magnesium comes from the lower carboniferous dolomites found in the studied area. Substitution of Mg^{2+} with Fe^{2+} is continuous; therefore the two minerals do not appear separately, which precludes their identification and study. Between the methods of study, the most significant for distinction between the pickeringite and halotrichite terms is the FT-IR and Raman spectroscopy; both of these methods were proven to be a powerful tool for highlighting of specific bands assumable to specific metal-oxygen vibrations.

The formation of gypsum in the two studied perimeters may be related to the oxidation of pyrite under the action of meteoric waters. Gypsum appears in the mass of metamorphic rock, which also contains small cubic relics of pyrite. On its turn, alunogen was formed by the reaction between the acidic solutions derived from the pyrite oxidation and Al-rich phases such as the (weathered) feldspars.

Acknowledgements

The authors wishes to present their gratitude for the support gained from the Geological Institute of Romania, peculiarly though the Microcosmos Laboratory and the laboratories of the National Geology Museum. We also would like to thank Dr. Ştefan Marincea, for a first review of the manuscript.

REFERENCES

Anthony J. W., Bideaux R. A., Bladh K.W. & Nichols M. C., 1990. *Handbook of Mineralogy*, Mineral data publishing, Tucson Arizona, USA, by permision of the Mineralogical Society of America;

Apopei I.A., Buzgar N., Damian Gh. & Buzatu A., 2014. *The Raman study of weathering minerals from the Coranda-Hondol open pit (Certej gold-silver deposit) and their photochemical degradation products under laser irradiation.* The canadian Mineralogist, Vol. 52, pp. 1027-1038;

Appleman D.E. & Evans H.T., Jr. 1973. *Indexing and least-squares refinement of powder diffraction data.* U.S. Geol. Surv., Comput. Contrib. 20 (NTIS Doc. PB-216);

Atoji M. & Rundle R.E., 1958. *Neutron diffraction study of gypsum.* $CaSO_4*2H_2O$, Journal of Chemical Physics, 29, 1306;

Ballirano P., 2006. *Crystal chemistry of the halotrichite group* $XAl_2(SO_4)_4 *22H_2O$*: the X=Fe-Mg-Mn-Zn compositional tetrahedron*, European Journal of Mineralogy, volume 18, 463-469;

Balintoni I., Balica C., Ducea M.N. & Hann H.P., 2014, *Peri-Gondwanan terranes in the Romanian Carpathians: A review of their spatial distribution,*

origin, provenance and evolution, Geoscience Frontiers, Geoscience frontieres 5, p. 395-411;

Benoit P.H., 1987. *Adaptation to microcomputer of the Appleman-Evans program for indexing and least-squares refinement of powder diffraction data for unit-cell dimensions.* American Mineralogist, Volume 72 (9-10), pages 1018-1019;

Berza T., Pop G., Seghedi A., Iancu V., Hîrtopanu I., Hîrtopanu P., Năstăseanu S. & Moisescu V., 1984, *Geological map of Romania, Scale 1:50000, 123b, Mount Oslea Sheet*, L-34-106-B, Geological Institute of Romania Ed.;

Berza T., Seghedi A., Pop Gr., Szasz L., Hârtopanu I., Săbău G., Moisescu V. & Popescu G., 1986, *Geological map of Romania, Scale 1:50.000, 106c Lupeni Sheet*, L-34-95-C, Geollogical Institute of Romania Ed.;

Brant A.R. & Foster R.W., 1959. *Magnesian Halotrichite from vinton county Ohio*, The Ohio Journal of Science 59(3):187.

Buzgar N., Buzatu A. & Sanislav I.V., 2009. *The Raman study on certain sulfates*, Analele Științifice ale Universității „Al. I. Cuza" IAȘI, Geologie. Tomul LV, nr. 1.

Cody D.R. & Bigss D.L., 1973. *Halotrichites szomolnokite and rozenite from Doluver State Park, Iowa, USA.* Canadian Mineralogist, Vol. ll, p. 958-970.

Cole W.F. & Lancucki C.J. 1973. *Hydrogen bonding in Gypsum.* Nature Physical science, 242, pp. 104-105;

Diaconu G., Marincea Ș., Dumitraș D.G., 2008. *Data on the Limanu cave mineralogy, South Dobrogea*, Trav. Instit. Speologic „Emil Racoviță", t. XLVII, p.65-77, București;

Dumitraș D-G., 2009. *Associations minerales dans les sediments de la grotte Cioclovina Uscată,* Diffusion ANRT, Saint –Etienne.

Fang, J.H. & Robinson, P.D., 1976. *Alunogen, $Al_2(H2O)_{12}(SO4)*35H_2O$: its atomic arrangement and water content.* American Mineralogist 61, 311–317.

Frost, R.L., Weier, M.L., Kloprogge, J.T., Rull, F. & Martinez-Frias, J., 2005. Raman spectroscopy of halotrichite from Jaroso, Spain. Spectrochimica Acta, 62 A, 176.180.

Hass, M. & Sutherland, G.B.B.M. 1956. *The IR spectra and crystal structure of gypsum.* Proceedings of the Royal Society of London, 236A, 427.445.

Innorta G., Rabbi E. & Tomadin L. 1980. *The gypsum-anhydrite equilibrium by solubility measurments.* Geochim Cosmochim Acta 44, pp. 1931-1936;

Košek F., Culka A., Žáček V. & Laufek F., 2018. *Native alunogen: A Raman spectroscopic study of a well-described specimen*, Journal of Molecular Structure 1157:191-200.

Lafuente B., Downs R.T., Yang H. & Stone N., 2015. The power of databases: The RRUFF project. Highlights in mineralogical Crystallography, Published by Walter de Gruyter GmbH, pp. 1-29, ISBN: 9783110417104;

Libowitzky, E., 1999. *Correlation of O-H stretching frequencies and O-H···O-H bond lengths in minerals*. Monatshefte für Chemie, 130, 1047.1059.

Locke, A.J., Martens, W.N. & Frost, **R.L.,** 2007. *Natural halotrichites - an EDX and Raman spectroscopic study*, Journal of. Raman Spetroscopy.

Lovas, G.A., 1986. *Structural study of halotrichite from Recsk (Mátra Mts., N-Hungary).* Acta Geologica Hungarica 29, 389–398.

Mastacan Gh. & Mastacan I., 1976. *Mineralogie, Vol II*, Editura Tehnică, București;

Nakamoto K., 2006. *Infrared and Raman spectra of inorganic and coordination compounds*, Published in the Handbook of Vibrational Spectroscopy, John Wiley & Sons Ltd, London;

Palmer S.J. & Frost R.L., 2006. *Synthesis and spectroscopic characterization of apjohnite and pickingerite*, Polyhedron 25 3379–3386.

Palmer S.J. & Frost R. L., 2011**.** *Molecular structure of Mg–Al, Mn–Al and Zn–Al halotrichites-type double sulfates—An infrared spectroscopic study*. Spectrochimica Acta Part A 78 1633–1639.

Palmer S.J., Reddy B.J. & Frost R.L., 2011. *Synthesis and vibrational spectroscopy of halotrichite and bilinite*, Spectrochimica Acta Part A 79 69–73.

Pedersen B. F. & Semmingsen D. 1982. Neutron diffraction refinement of the structure of the gypsum, $CaSO_4*2H_2O$. Acta Crystallographica, B38, pp. 1074-1077;

Popescu C. Gh. & Constantinescu E., 1982. *Pyrophyllite from anchimetamorphic schist in the Parâng Mountains, South Carpathians, Romania; Petrogenetic significances.* Published in: Crystal Chemistry of Minerals – Proceedings of the 13th General Meeting of IMA, September 19-25, 1982, Varna, p. 675 – 690;

Quartieri, S., Triscari, M. & Viani, A., 2000. *Crystal structure of the hydrated sulphate pickeringite $MgAl_2(SO_4)_4*22\ H_2O$: X-ray powder diffraction study.* European Journal of Mineralogy 12, 1131–1138.

Ross S.D., 1974. *The Infrared Spectra of Minerals*, The Mineralogical Society London, in: V.C. Farmer (Ed.), p. 423 (Chapter 18).

Seidl V., Knop O. & Falk M., 1969. *Infrared studies of water in crystalline hydrates: gypsum $CaSO_4*2H_2O$*, Canadian journal of Chemistry, 47, 1361;

Žáček V., 1988. *Zonal association of secondary minerals from burning dumps of coal mines near Kladno, Central Bohemia, Czechoslovakia*, Acta Univ. Carol. Geol. 3, pag 315-341.

Received at: 13. 03. 2020

Revised at: 15. 06. 2020
Accepted for publication at: 25. 06. 2020
Published online at: 03. 07. 2020